Macromolecules

ARTICLE

pubs.acs.org/Macromolecules

Structure and Dynamics of Zinc-Neutralized Sulfonated Polystyrene Ionomers

Alicia M. Castagna,[†] Wenqin Wang,[‡] Karen I. Winey,[*,‡] and James Runt[*,†]

[†]Department of Materials Science and Engineering, The Pennsylvania State University, University Park, Pennsylvania 16802, United States

[‡]Department of Materials Science and Engineering, University of Pennsylvania, Philadelphia, Pennsylvania 19104, United States

Supporting Information

ABSTRACT: Scanning transmission electron microscopy (STEM), X-ray scattering, and dielectric relaxation spectroscopy were used to investigate the structure and dynamics of Zn-neutralized sulfonated polystyrene (SPS) ionomers. STEM and X-ray scattering revealed the presence of spherical aggregates ~2 nm in diameter. Successful fitting of scattering data to the Kinning − Thomas modified hard sphere model provided information on aggregate diameter, radius of closest approach, and number density. The analysis revealed that aggregate size is independent of degree of sulfonation and neutralization level, and that aggregate composition becomes increasingly ionic with increasing neutralization. Two segmental relaxations were identified in dielectric loss spectra corresponding to cooperative motion of chain segments in the matrix and motions of segments restricted by aggregates. Additionally, a Maxwell−Wagner−Sillars interfacial polarization process was revealed, with relaxation times in good agreement with predictions from a simple spherical polarization model.

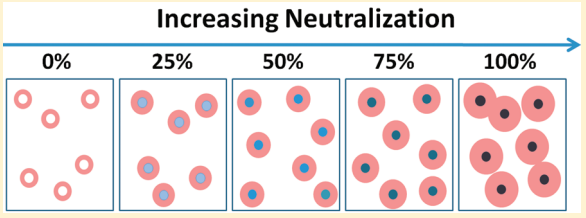

INTRODUCTION

Incorporating small fractions (typically <10 mol %) of ionic groups into polymer chains has been shown to have profound effects on thermal, mechanical, and charge transport properties.[1,2] These ionomers are used in a range of applications including performance coatings, packaging, membranes, and actuators. Ionic species tend to self-assemble into microphase-separated domains due to Coulombic interactions that serve as thermoreversible cross-links.

Although ion aggregation and properties of ionomers have been studied extensively using a number of different techniques (including dynamic mechanical analysis (DMA),[3−5] rheology,[6] X-ray and neutron scattering,[2,7−11] and scanning transmission electron microscopy (STEM)[2,11−13]) little is known about the effect of these ionic clusters on the molecular dynamics of this class of materials. Dielectric relaxation spectroscopy has been used to investigate the dynamics of some ionomers, predominantly on poly(styrene-*co*-methacrylic acid) and poly(ethylene-*co*-methacrylic acid) ionomers,[1,14,15] but very little has been done on sulfonated polystyrene.[16,17] We intend to elucidate the connection between aggregate morphology and dynamics by applying an integrated and systematic approach using sulfonated polystyrene (SPS) as a model ionomer.

In our previous paper, we demonstrated that sulfonation has an important effect on the structure and dynamics of sulfonated polystyrene acid copolymers (having 3.5, 6.7, and 9.5 mol % sulfonation), the precursors to the ionomers investigated herein.[18] In this publication we will focus on the effect of neutralizing these materials with zinc. In our investigation, morphology was characterized using X-ray scattering and scanning transmission electron microscopy (STEM) while the dynamics were investigated using dielectric relaxation spectroscopy (DRS).

EXPERIMENTAL SECTION

Sample Preparation. Atactic polystyrene, purchased from Pressure Chemical (M_w = 123 kg/mol, PDI = 1.06), was sulfonated according a previously published procedure.[18] SPS acid copolymers were neutralized by dissolving in a 90/10 v/v mixture of toluene/methanol. A stoichiometric amount of Zn acetate was dissolved in a 50/50 v/v mixture of toluene/methanol and added slowly into the gently agitated SPS solution to achieve different degrees of neutralization. The reaction was held at 50 °C for 2 h. In this publication the ionomers are designated as SPS*x*-*y*Zn, where *x* is the mole fraction of sulfonation (3.5, 6.7, or 9.5) and *y* is the percent neutralization (0, 25, 50, 75, and 100).

The neutralized ionomers were solvent cast at ambient conditions, air-dried for 1−2 days, and then dried under vacuum at 120 °C for at least 24 h. Ionomers with T_g around or above 120 °C (SPS6.7-*y*M and SPS9.5-*y*M) were further annealed at ~ T_g + 20 °C for another day. The dried ionomer films were then hot pressed at 160 °C and used for X-ray scattering, STEM imaging, and dielectric spectroscopy. All materials

Received: January 23, 2011
Revised: February 24, 2011
Published: March 29, 2011

dx.doi.org/10.1021/ma2001614 | *Macromolecules* 2011, 44, 2791–2798

were stored in vacuum desiccators prior to characterization. Selected samples were sent to the Galbraith Laboratories for elemental analysis to determine the percent neutralization. The results were consistent with the stoichiometric neutralization levels within experimental error (<5%).

Thermal Analysis. Glass transition temperatures (T_g) were determined using a TA Instruments Q2000 differential scanning calorimeter (DSC). The response was measured over the temperature range 40−180 °C at a heating rate of 10 °C/min under a nitrogen flow of 50 mL/min. The T_g was taken as the inflection point in the DSC thermogram from the second heating scan.

Fourier Transform Infrared Spectroscopy (FTIR). Samples were prepared for FTIR spectroscopy by hot pressing into thin films at 160 °C. FTIR spectra were collected at a resolution of 2 cm^{-1} using a Nicolet 450 FT-IR equipped with an MCT/B detector. A total of 256 scans were signal averaged at room temperature.

Scanning Transmission Electron Microscopy. STEM specimens were sectioned from the solvent-cast, dried, annealed, and hot pressed ionomer films at room temperature using a Reichert-Jung ultramicrotome with a diamond knife to a nominal thickness of 30−50 nm. STEM experiments were performed using a JEOL 2010F field emission transmission electron microscope. High-angle annular dark field (HAADF) images were recorded using a 0.7 nm STEM probe and a 70 μm condenser aperture at an accelerating voltage of 200 keV.

X-ray Scattering. X-ray scattering experiments were performed with a multiangle X-ray scattering (MAXS) apparatus using Cu K_α X-rays generated from a Nonius FR 591 rotating-anode generator operated at 40 kV and 85 mA. The bright, highly collimated beam was obtained via Osmic Max-Flux optics and triple pinhole collimation under vacuum. The scattering data were collected using a Bruker Hi-Star multiwire detector with sample-to-detector distances of 11, 54, and 150 cm. The isotropic 2-D data were integrated into 1D plot using *Datasqueeze* software.[19]

The scattering data of the SPS ionomers were fit to:

$$I(q) = I_{KT}(q) + L_1(q) + L_2(q) + C \quad (1)$$

where $I_{KT}(q)$ is the Kinning−Thomas (K−T) modified hard-sphere model,[11,20] $L_1(q)$ and $L_2(q)$ are Lorentzian functions used to fit the two polystyrene amorphous halos in the wide angle region, and C is a constant used to account for the instrumental background scattering, as previously reported.[21]

Dielectric Relaxation Spectroscopy. Samples 0.2−0.4 mm thick were sandwiched between brass electrodes with a top electrode diameter of 2 cm. Isothermal relaxation spectra were collected under nitrogen using a Novocontrol GmbH Concept 40 DRS spectrometer from 0.01 Hz to 10 MHz on heating from 10 to 220 °C.

Dielectric strength ($\Delta\varepsilon$) and characteristic relaxation time (τ_{HN}) were determined for each relaxation process by fitting the dielectric loss to the appropriate form of the Havriliak Negami (HN) function:

$$\varepsilon^*_{HN}(\omega) = \frac{\Delta\varepsilon}{(1 + (i\tau_{HN}\omega)^a)^b} \quad (2)$$

where a and b are shape parameters. The characteristic relaxation time is related to the maximum frequency of maximum loss by:

$$f_{max} = \left[\frac{1}{2\pi\tau_{HN}}\right]\left[\frac{\sin(\pi a/(2+2b))}{\sin(\pi ab/(2+2b))}\right]^{1/a} \quad (3)$$

Above T_g, the contribution from ohmic conduction dominates the loss contribution (ε''), potentially masking dipolar processes. This conduction contribution is not manifested in the real part of the dielectric response (ε') and using a numerical approach one can calculate the conduction free loss from ε'. We chose to apply the straightforward derivative method to achieve this, where the ohmic-conduction-free loss is determined from the logarithmic derivative of the dielectric constant:[22,23]

$$\varepsilon''_D = -\frac{\pi}{2}\frac{\partial\varepsilon'(\omega)}{\partial[\ln\omega]} \quad (4)$$

Wubbenhorst et al. have shown that this method is a very good approximation of the conduction-free loss.[23] The appropriate

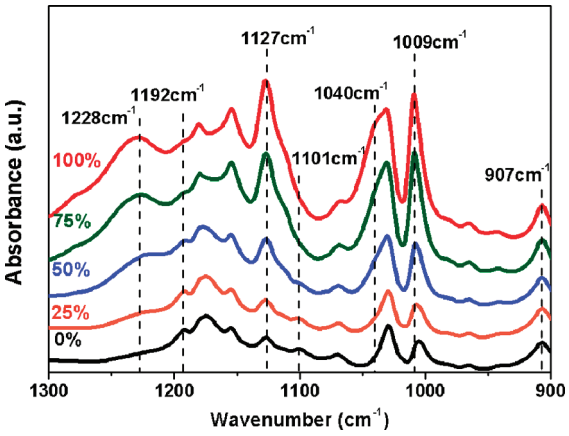

Figure 1. FTIR absorbance spectra for SPS9.5-0, -25, -50, -75, and -100Zn in the region 1300−900 cm^{-1}. Spectra are shifted vertically for clarity.

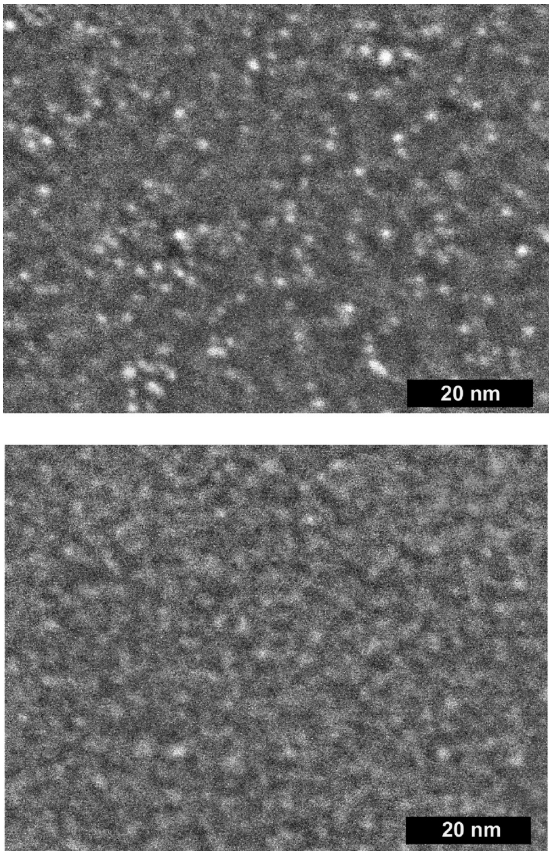

Figure 2. Representative HAADF STEM images of SPS6.7-100Zn (top) and SPS9.5-100Zn (bottom) show a uniform distribution of spherical ionic aggregates.

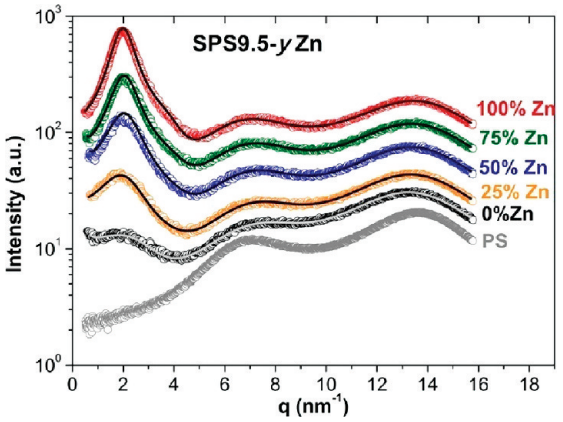

Figure 3. X-ray scattering intensity vs scattering vector q for polystyrene and SPS9.5-0, -25, -50, -75, and -100Zn (symbols) and the corresponding best fit of the scattering data using eq 1 (lines). The data were vertically shifted for clarity.

derivative form of the HN function was used to fit processes resolved by this method.[23]

RESULTS AND DISCUSSION

FTIR. The state of neutralization was investigated for SPS9.5-0, -25, -50, and -100Zn using FTIR. In particular, the region between 1300−900 cm^{-1} clearly reveals changes in the sulfonate stretching bands (Figure 1). The bands at ∼1228 and 1039 cm^{-1} correspond to the asymmetric and symmetric stretching vibrations of S−O bonds in $-SO_3M$, respectively, where M is the Zn ion.[17,24] As expected, the SO_3M band increases in relative intensity upon neutralization while the S−O band is unaffected. The absorptions at 1127 and 1009 cm^{-1} result from the in-plane skeletal vibration of benzene rings substituted by SO_3^- and SO_3M, both of which increase in relative intensity upon neutralization.[17,24] The apparent increase in free anions (i.e., the benzene SO_3^- band) is likely due to charge delocalization within the aggregates which effectively screens the presence of the ions, making it appear to the benzene ring vibrations as though the SO_3^- groups are uncoordinated. The absorbance at 1101 cm^{-1} (skeletal vibration of benzene rings substituted by SO_3H) becomes indistinct upon ion substitution.[24,25] As expected the doublet at ∼1200 cm^{-1} and the band at 1040 cm^{-1} (asymmetric and symmetric stretching of the $-SO_3^-$ Zn, respectively) increased in relative intensity.[17,24] These trends are all indicative of the successful, systematic neutralization of the sulfonic acid groups.

Morphology. Spherical, uniformly distributed bright features, corresponding to Zn-rich ionic aggregates within a matrix of lower average atomic number, are observed in HAADF STEM images of the SPS ionomers (Figure 2). The diameters of the aggregates were determined by the full width at half-maximum (fwhm) of the Gaussian functions fit to the intensity profiles taken across individual bright features.[21] Taking into account the extensive projection overlap in the STEM images[26] and the limit of instrumental resolution, STEM images indicate that the diameters of ionic aggregates are ∼2 nm and independent of sulfonation level.

Representative scattering profiles for the SPS9.5-0, -25, -50, -75, and -100Zn ionomers are displayed in Figure 3. Three isotropic maxima are observed: the polystyrene amorphous halo

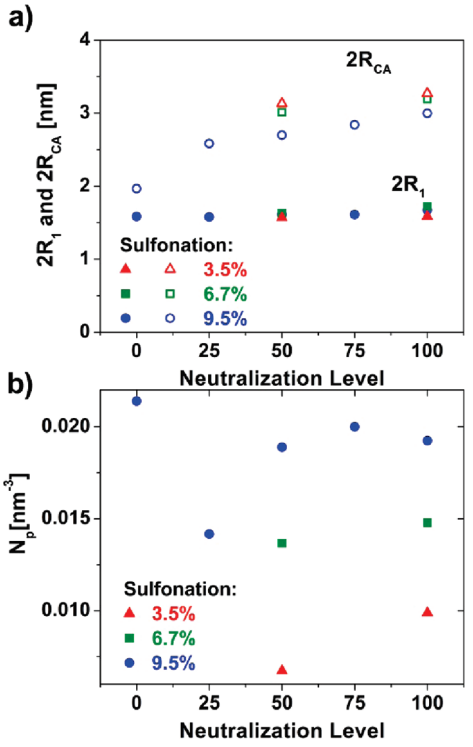

Figure 4. (a) $2R_1$ (symbols) and $2R_{CA}$ (open symbols) and (b) N_p as a function of neutralization level determined by fitting the SPSx-yZn scattering data to eq 1.

(∼13 nm^{-1}), the polystyrene polymerization peak (∼7 nm^{-1}),[27] and the aggregate peak (1−2 nm^{-1}). The scattering intensity of the aggregate peak was found to significantly increase with increasing neutralization, which is consistent with enhanced electron density contrast as Zn ions are incorporated into the clusters. The K−T modified hard sphere model was used to facilitate the interpretation of this maximum. The model assumes that this peak arises from interparticle scattering from monodisperse, spherical aggregates homogeneously distributed in the polymer matrix of lower electron density. Four parameters are utilized to characterize aggregation: the aggregate radius R_1, the radius of closest approach R_{CA}, the number density of the aggregates N_p, and the amplitude A of the scattering maxima.[11] Zhou et al. have demonstrated that the size and number density of ionic aggregates in lightly sulfonated SPS ionomers observed in STEM and determined from fitting the X-ray scattering data quantitatively agree.[11]

Equation 1 provides a good fit to the scattering data (Figure 3) and the corresponding K−T fit parameters (R_1, R_{CA}, and N_p) are displayed in Figure 4 for each sulfonation and neutralization level. Degree of sulfonation did not have a substantial effect on aggregate size, or R_{CA}, but a substantial increase in N_p is observed. Degree of neutralization also does not have an appreciable effect on aggregate size, while R_{CA} systematically increases. Previous studies on poly(styrene-*co*-methacrylic acid)−Cu ionomers[28] and SPS-Zn ionomers[8] also showed that the size of the ionic aggregates is independent of acid content and neutralization level. These results suggest that the size of ionic aggregates in those strongly segregated ionomers is mainly controlled by the chemical structure of the acid copolymer, i.e., polymer backbone and acid type.

dx.doi.org/10.1021/ma2001614 |*Macromolecules* 2011, 44, 2791–2798

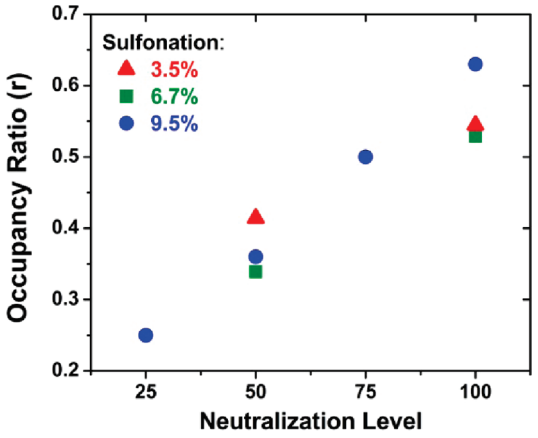

Figure 5. Occupancy ratio of the ionic aggregates (r) determined from N(cation, N_p)/N(cation, R_1) as a function of neutralization level for SPSx-yZn.

The increase in scattering intensity, the weak increase in the radius of closest approach and independence of aggregate size with degree of neutralization suggest that the composition within the ionic aggregates is changing as zinc ions are added. To further elucidate this change, the approximate number of cations incorporated into an average aggregate can be calculated using R_1 or N_p. The number of cations can be determined from R_1 using

$$N(\text{cation}, R_1) = \frac{4}{3}\pi {R_1}^3 \left(\frac{n_{\text{sulfate}}}{n_{\text{pair}}}\right)\left(\frac{N_A \rho_{\text{sulfate}}}{M_{\text{sulfate}}}\right) \quad (5)$$

where the volume of $Zn^{2+}(SO_3^-)_2$ is approximated using the atomic density (ρ), and formula molar mass (M) of zinc sulfate ($ZnSO_4$) and the ratio of the number of atoms in the zinc sulfate and the ion pair. This calculation assumes that ionic aggregates consist entirely of ionic groups.[11] The number of cations per aggregate was also determined from N_p using

$$N(\text{cation}, N_p) = \frac{1}{p}\frac{N_A \rho_{\text{SPS}}}{M_{\text{SPS}} N_p}\varphi_{\text{acid}}\frac{y}{100} \quad (6)$$

where p is the valency number, ρ_{SPS} and M_{SPS} are the density and the monomeric molar mass of SPS, respectively, φ_{acid} is the volume fraction of sulfonic acid, and y is the percent of neutralization. It is assumed, in this calculation, that all ions are incorporated into aggregates, thus representing the upper limit of cation availability in an average volume of $V_p = 1/N_p$.[11]

From N_p and R_1 one can determine the occupancy ratio, r = N(cation, N_p)/N(cation, R_1), which quantifies aggregate composition.[26] A value of $r > 1$ corresponds to an excess of ionic groups, i.e. more ionic groups are available than can be accommodated by the volume of ionic aggregates. A value of $r < 1$ indicates a deficit of ionic groups; i.e., the aggregates are less dense than the corresponding metal sulfate.

The occupancy ratio of the ionic aggregates (Figure 5) in these ionomers is less than 1 at all sulfonation and neutralization levels and does not change significantly with sulfonation level, but increases systematically with increasing neutralization. This suggests that more zinc sulfonate groups are incorporated into ionic aggregates upon Zn neutralization; i.e., the aggregates are becoming more ionic.

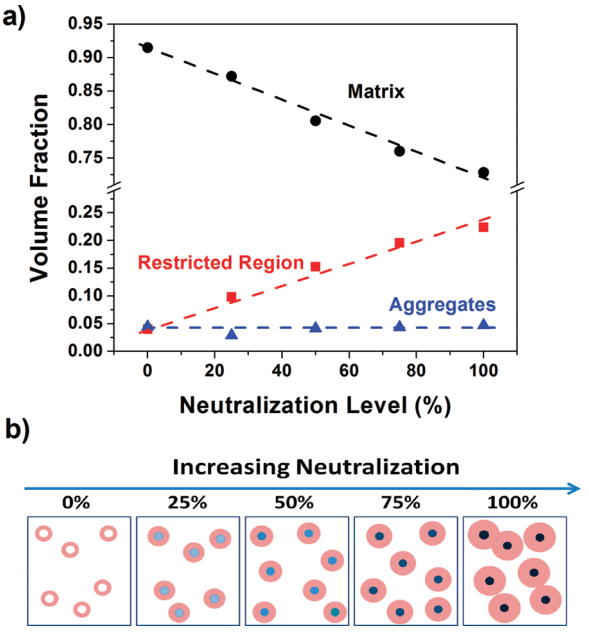

Figure 6. (a) Volume fraction of the region of restricted mobility (φ_{RR}), aggregates (φ_A) and matrix ($1 - \varphi_{RR} - \varphi_A$) as a function of degree of neutralization for SPS9.5-yZn and (b) illustration of neutralization effect on volume fraction.

From this result it follows that, for a fixed aggregate size, the region around the aggregates contains more polystyrene chain segments tethered to the aggregate by their anion resulting in a less mobile region of restricted mobility. As theorized by Eisenberg et al., the mobility of the monomeric segments drops off significantly in the region of restricted mobility near the aggregate.[1,5,29] Eisenberg et al. have estimated the length scale of the restricted region to be on the order of the persistence length of the polymer chain (~1 nm for PS),[29] which is on the order of $R_{CA} - R_1$. The volume fractions of the restricted region (φ_{RR}) and aggregates (φ_A) can be estimated using R_1, R_{CA}, and N_p:

$$\varphi_{RR} = \frac{4}{3}\pi({R_{CA}}^3 - {R_1}^3)N_p \quad (7)$$

$$\varphi_A = \frac{4}{3}\pi {R_1}^3 N_p \quad (8)$$

With increasing degree of neutralization, φ_{RR} increases, corresponding to a decrease in the unrestricted matrix, while φ_A remains constant (Figure 6). The matrix is composed primarily of polystyrene chain segments, but also likely contains unneutralized acid species when the ionomers are partially neutralized. This estimate of the changes in the volume of the restricted region will be critical in the interpretation of the dynamics, as follows.

Segmental and Slow Segmental Dynamics. The segmental relaxation (α) corresponds to the cooperative motion of chain segments and is related to the glass transition. In our previous investigation of the precursor SPS acid copolymers we found that increasing sulfonic acid content slowed down the α relaxation time, consistent with the observed increase in T_g.[18] Despite only one very broad T_g observed in DSC, a second slow segmental process (α_2) is clearly evident in the dielectric spectra upon neutralization with Zn (Figure 7a), at frequencies 1−4 decades lower than the α relaxation. In a previous study on similar SPS

dx.doi.org/10.1021/ma2001614 |*Macromolecules* 2011, 44, 2791–2798

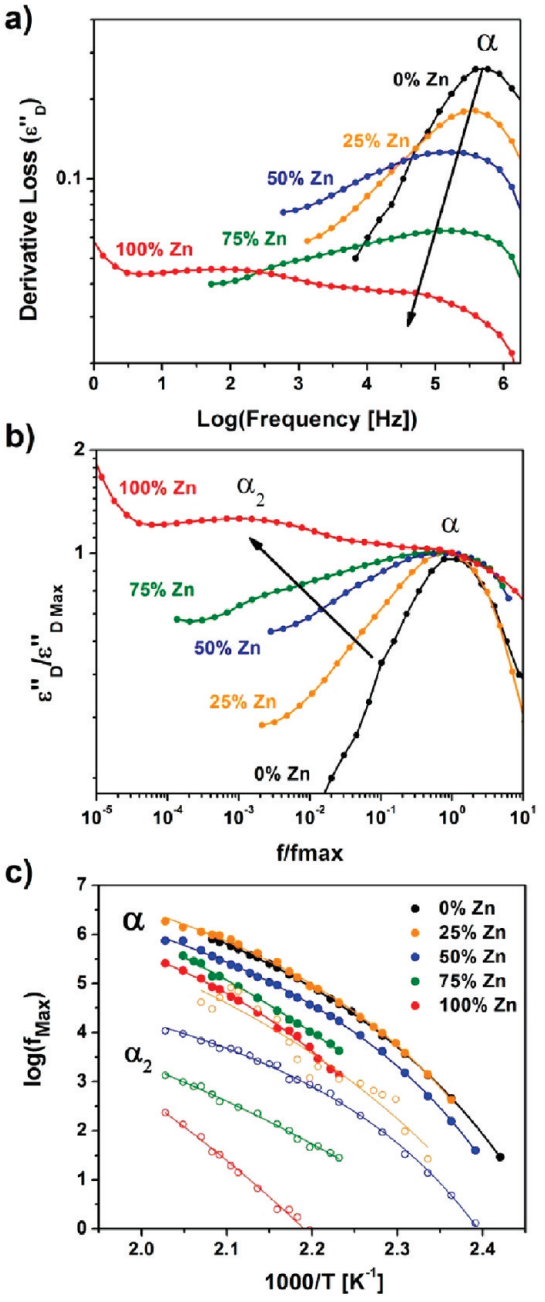

Figure 7. (a) Conduction free loss at $\sim T_g + 80$, (b) normalized conduction free loss $\sim T_g + 80$, and (c) relaxation frequency of α (filled symbols) and α_2 (open symbols) including VFT fits (lines) for SPS 9.5-*y*Zn at 0, 25, 50, 75, and 100% neutralization.

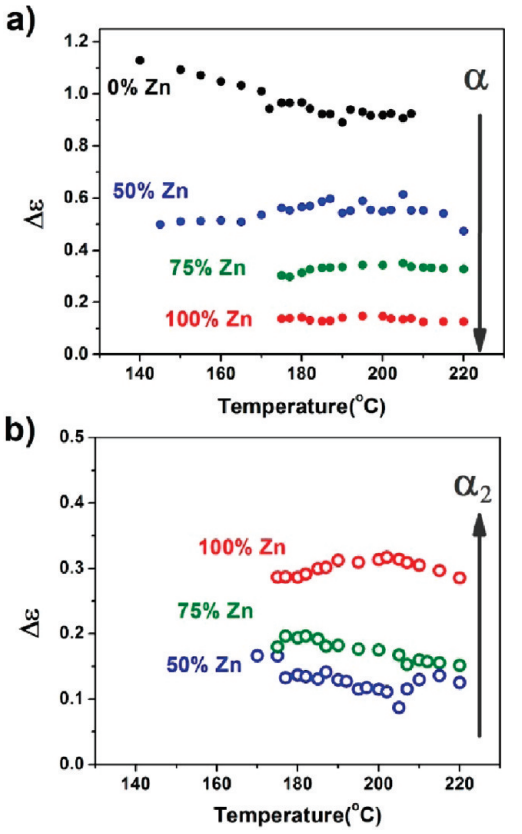

Figure 8. Dielectric strength of (a) α (filled symbols) and (b) α_2 (open symbols) for SPS 9.5-*y*Zn at 0, 25, 50, 75, and 100% neutralization.

ionomers, two relaxations were observed in dynamic mechanical analysis (DMA) experiments.[17] The DMA α process corresponds with the α relaxation from DRS, and a relaxation attributed to the motion of chain segments associated with the aggregates was observed at temperatures higher than those measured in our DRS experiments (~275 °C for Zn neutralized SPS).[17]

Effect of Neutralization. With increasing neutralization we find that the α_2 process shifts systematically to lower frequencies and increases in strength, while the α relaxation also slows but decreases in strength (Figure 7). These changes occur concurrently as φ_{RR} increases and the volume fraction of matrix chain segments subsequently decreases. As a consequence, we attribute the origin of α_2 to chain segments whose mobility are restricted by the presence of aggregates, while the α relaxation corresponds to the motion of relatively unhindered segments. This α_2 process is observed at temperatures much lower than the second process (noted above) observed in DMA experiments.[17]

As neutralization increases and the aggregates become increasingly more ionic, the chain segments adjacent to the aggregates become less mobile as the chains are bound tighter to the aggregate, which would further reduce segment mobility and increase the α_2 relaxation time. This is supported by the shift to lower frequencies (longer times) of α_2, Figure 7c. Additionally the α process shifts to lower frequencies as the network becomes increasingly restricted by the cross-linking effect of the aggregates. The temperature dependence of both processes follows a Vogel−Fulcher−Tammann (VFT) form:

$$f = f_0 \exp\left(\frac{B}{T - T_0}\right) \tag{9}$$

where T_0 is the Vogel temperature, f_0 is associated with vibration lifetimes,[30] and the temperature coefficient B is related to the apparent activation energy ($E_a = BR/([1 - T_0]/T)^2$).[22] The dynamic T_g (T_{ref}) is determined by extrapolating the VFT fit to $\tau = 100$ s ($f = 0.00159$ Hz). T_{ref} of the α process and the calorimetric T_g are within experimental error; $T_{ref}(\alpha)$, $T_{ref}(\alpha_2)$, and the DSC T_g are reported in the Supporting Information (Table S1).

dx.doi.org/10.1021/ma2001614 |*Macromolecules* 2011, 44, 2791–2798

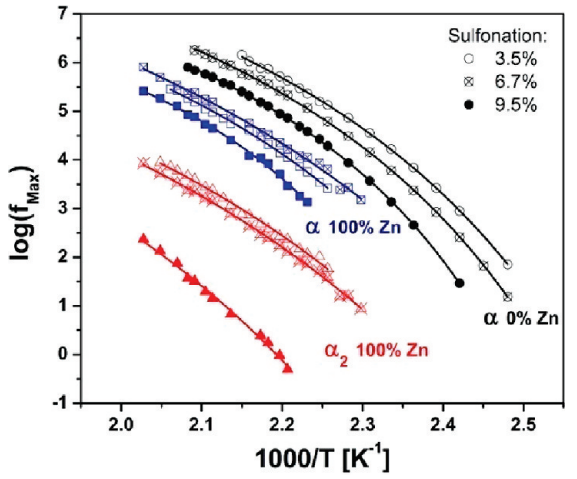

Figure 9. Sulfonation effects on the relaxation frequency of α and α_2 for SPS3.5 (open symbols), 6.7 (crossed symbols), and 9.5 (filled symbols) for unneutralized (black circles) and 100% Zn neutralized (blue squares, α; red triangles, α_2). Solid lines are fits to the VFT equation.

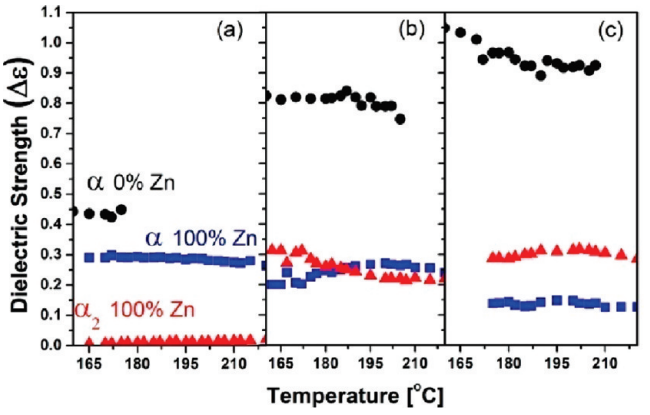

Figure 10. Sulfonation effects on Δε of α and α_2 for (a) SPS3.5, (b) 6.7, and (c) 9.5 for unneutralized (black circles) and 100% Zn (blue squares, α; red triangles, α_2).

As neutralization level increases the strength of the α process decreases (Figure 8a), consistent with a decrease in acid groups in the matrix region. At full neutralization (elemental analysis showed that the neutralization level is 100% within 5% experimental error) no acid groups remain in principle, yet the strength of this process (~0.1) is still significantly greater than that of PS (~0.03). It is possible that a small number of acid groups remain unneutralized and/or some small fraction of neutralized ionic species are kinetically or sterically trapped in the matrix.

The origin of strength of the α_2 processes is less straightforward. From Eisenberg's model of ionic aggregation, one would expect that the region of restricted mobility would consist of polystyrene chain segments and therefore the strength of this process would be similar to that of PS.[1,5,29] However, the strength of the α_2 process (0.1−0.3, Figure 8b) is clearly much greater than that of polystyrene. There are several possible sources for the enhanced strength of this process. It is possible that small scale dipolar motion of the ion pair within the aggregate which pins the chain segments in this region could contribute to the dipole moment of this relaxation. Additionally, it is typically assumed that the aggregates have no net dipole moment (all dipoles cancel), however it is possible that there is some small contribution owing to misalignments and dynamic motion of the aggregate. A further possibility is the presence of ion pairs or sulfonic acid groups (at partial neutralization) in the region of restricted mobility. In the Eisenberg-Hird-Moore model this region is expected to be depleted of ions due to the high electrostatic forces the ions would experience close to the aggregate,[29] however, it is possible that ionic groups could be kinetically or sterically hindered from participating in aggregates. It is likely that the enhanced α_2 strength arises from some combination of these sources.

Effect of Degree of Sulfonation at 100% Neutralization. In our previous investigation of the SPS acid copolymer precursors we demonstrated that the relaxation frequencies of the segmental process decreased systematically with increasing sulfonic acid content.[18] The effect of sulfonation on the relaxation frequencies for the Zn neutralized ionomers is somewhat more complex, as illustrated in Figure 9. The α and α_2 frequency maxima of SPS3.5−100Zn and SPS6.7−100Zn are not significantly different, but these processes shift to lower frequencies for SPS9.5−100Zn, particularly α_2. As the number density of acid groups increases the average polymer segment length between aggregates is expected to decrease as the average chain separation of acid groups decreases. As a result, the mobility of these chains is expected to decrease resulting in the increase in relaxation time (Figure 9). This effect is similar to the increase in T_g observed in rubbers as the segment length in between cross-linking points decreases.[31]

The relative strengths of the α and α_2 relaxations (Figure 10) change with degree of sulfonation in the fully neutralized ionomers: α dominates at 3.5% sulfonation, α roughly equals α_2 at 6.7%, and α_2 dominates at 9.5%. Since φ_{RR} increases with increasing degree of sulfonation (see Supporting Information, Figure S1) as the number density of aggregates increases, the fraction of chains participating in regions of restricted mobility increases, resulting in the relative increase in the strength of α_2.

Maxwell−Wagner Sillars Interfacial Polarization. In our previous work we identified the Maxwell−Wagner Sillars interfacial polarization process in dielectric spectra of SPS9.5 and SPS6.7, both of which were demonstrated to exhibit acid group aggregation.[18] This relaxation arises from space charge accumulation at boundaries between phases in an inhomogeneous media.[32,33] It is also observed for the Zn neutralized ionomers (Figure 11) and is highly sensitive to the degree of neutralization.

In an attempt to understand the neutralization dependence of the MWS process, we apply a simple composite model.[32] The matrix and filler (aggregates) are assumed to have frequency independent dielectric constants and conductivities (ε_m, σ_m and ε_f, σ_f, respectively) yielding a Debye-like relaxation process:

$$\varepsilon^*(\omega) = \varepsilon'(\omega) - i\varepsilon''(\omega) = \varepsilon_\infty + \frac{\Delta\varepsilon}{1 + i\omega\tau} \qquad (10)$$

where ε_∞ is the high frequency limit of the real part (ε') of the complex dielectric constant (ε^*).[32] Using the Debye approximation, the theoretical relaxation time of the MWS process can be estimated using:

$$\tau_{MWS} = \varepsilon_0 \frac{(1-n)\varepsilon_m + n\varepsilon_f + n(\varepsilon_m - \varepsilon_f)\varphi_f}{(1-n)\sigma_m + n\sigma_f + n(\sigma_m - \sigma_f)\varphi_f} \qquad (11)$$

where ε_0 is the vacuum permittivity, n is a shape factor, and φ_f is the volume fraction of filler particles.[32] A predicted relaxation

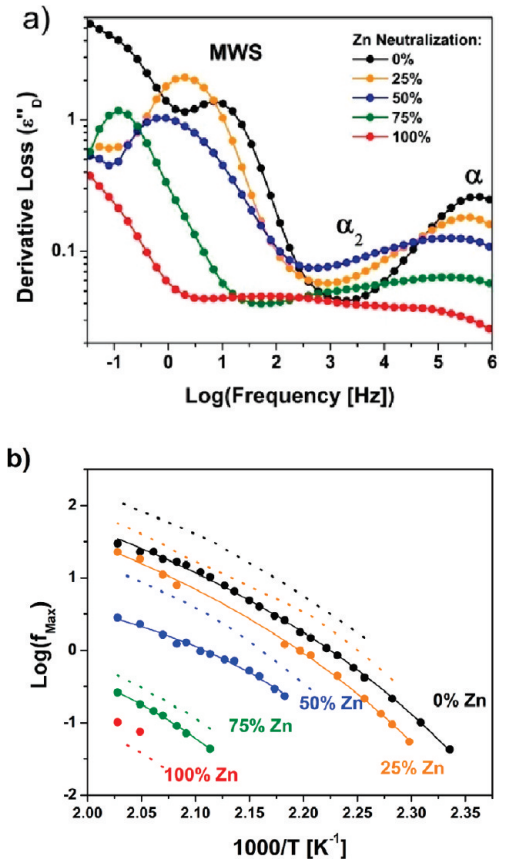

Figure 11. (a) Derivative loss spectra at T_g + 80 °C and (b) temperature dependence of the MWS relaxation frequency (filled symbols) including fits to the VFT equation (solid lines) and the relaxation frequency predicted from eq 11 (dotted lines) for SPS9.5-0, -25, -50, -75, and -100Zn.

time was calculated for our ionomers for the case where $\varepsilon_m = \varepsilon_{PS}$, σ_m is the experimental dc conductivity (see Supporting Information, Figure S2), $n = {}^1/_3$ (spherical shape factor), and $\varphi_f \approx 0.05$ (from Figure 6). The filler conductivity (σ_f) is assumed to be negligible in the temperature range of the current experiments and the dielectric constant of the filler (ε_f) is calculated from the refractive indices (η) of H_2SO_4 and $ZnSO_4$[34] for the acid and zinc ionomers, respectively ($\varepsilon = \eta^2$).

The temperature dependence of the dc conductivity and experimental relaxation frequency of the MWS process follow a VFT temperature dependence with temperature coefficients (B) which are within error (Supporting Information, Figure S2, and 11b, respectively). The predicted relaxation times from eq 11 follow an almost identical temperature dependence and are within a ${}^1/_2$-decade of frequency of the experimental data (Figure 11b), further supporting the origin of this process. The dielectric constants and filler fraction in eq 11 are kept constant and therefore changes in the relaxation time due to neutralization are dictated by the dc conductivity, which decreases with increasing neutralization owing to an increase in T_g and reduced chain mobility discussed previously. The dielectric strength, discussed in the Supporting Information, is not predicted adequately by this simple model owing largely to the assumption of zero conductivity in the filler particles.

SUMMARY

The morphology and dynamics of Zn neutralized SPS ionomers were investigated by integrating results from FTIR spectroscopy, STEM, X-ray scattering and dielectric relaxation spectroscopy. X-ray scattering and STEM revealed spherical aggregates ~2 nm in diameter. The size of these aggregates was found to be independent to the extent of sulfonation and degree of neutralization of these ionomers. Successful fitting of the X-ray data to the Kinning−Thomas modified hard sphere model further revealed that the number density of aggregates increased with increasing sulfonation but only weakly with degree of neutralization, while the radius of closest approach decreased with increasing sulfonation but increased with increasing neutralization. It was interpreted that the aggregates are becoming more ionic with increasing neutralization. The volume fraction of the aggregates and restricted region (assuming that the radius of the restricted region is equal to the radius of closest approach) were determined from R_A, R_{CA}, and N_p values extracted from the scattering model. These observations and calculations were critical in the interpretations and calculations of dynamics from the DRS results.

Two segmental processes were observed, α and α_2, which were ascribed to originate from the relatively unrestricted matrix cooperative chain motion and the motion of chains near the ionic aggregates. Both the α and α_2 relaxation times increase with increasing neutralization level (at 9.5% sulfonation) and with sulfonation level (at 100% neutralization). This increase is more dramatic for α_2 as the ionic aggregates become more ionic and the mobility of adjacent chain segments is substantially reduced. Furthermore, the dielectric strength of the two segmental relaxations correlate well with the relative amounts of matrix and restricted regions as a function of neutralization level and acid content. Additionally, a high temperature process was revealed after removing the dc conductivity contribution to the loss. This process, which was also observed in the precursor microphase-separated acid copolymers, was modeled as an interfacial polarization process using a simple spherical model. The predicted relaxation times were found to agree remarkably well with the experimental data.

The combination of experimental tools used in this study provides a highly reliable and self-consistent interpretation of the morphology and dynamics of these complex polymers. In a future manuscript the structure and dynamics of SPS neutralized with monovalent ions (Na and Cs) will be detailed to further define the effect of ion type on the structure and dynamics of these materials.

ASSOCIATED CONTENT

Supporting Information. Volume fraction of the region of restricted mobility with sulfonation, T_{ref} for α and α_2, DSC T_g, dc conductivity, and Maxwell−Wagner Sillars interfacial polarization—strength and model limitations. This material is available free of charge via the Internet at http://pubs.acs.org.

ACKNOWLEDGMENT

This research was supported by the U.S. Department of Energy, Office of Basic Energy Sciences, Division of Materials Sciences and Engineering under Award DEFG02-07ER46409 and by the NSF, Polymer Program under Award NSF05-49116.

We also thank Dr. Kevin Masser and Dr. Paul Painter for their helpful discussions.

REFERENCES

(1) Eisenberg, A.; Kim, J.-S. *Introduction to Ionomers*; Wiley: New York, 1998.
(2) Grady, B. P. *Polym. Eng. Sci.* **2008**, *48*, 1029–1051.
(3) Weiss, R. A.; Fitzgerald, J. J.; Kim, D. *Macromolecules* **1991**, *24*, 1071–1076.
(4) Weiss, R. A.; Yu, W. C. *Macromolecules* **2007**, *40*, 3640–3643.
(5) Hird, B.; Eisenberg, A. *Macromolecules* **1992**, *25*, 6466–6474.
(6) Colby, R. H.; Zheng, X.; Rafailovich, M. H.; Sokolov, J.; Peiffer, D. G.; Schwarz, S. A.; Strzhemechny, Y.; Nguyen, D. *Phys. Rev. Lett.* **1998**, *81*, 3876.
(7) Earnest, T. R.; Higgins, J. S.; Handlin, D. L.; MacKnight, W. J. *Macromolecules* **1981**, *14*, 192–196.
(8) Yarusso, D. J.; Cooper, S. L. *Macromolecules* **1983**, *16*, 1871–1880.
(9) Weiss, R. A.; Lefelar, J. A. *Polymer* **1986**, *27*, 3–10.
(10) Ding, Y. S.; Hubbard, S. R.; Hodgson, K. O.; Register, R. A.; Cooper, S. L. *Macromolecules* **1988**, *21*, 1698–1703.
(11) Zhou, N. C.; Chan, C. D.; Winey, K. I. *Macromolecules* **2008**, *41*, 6134–6140.
(12) Winey, K. I.; Laurer, J. H.; Kirkmeyer, B. P. *Macromolecules* **2000**, *33*, 507–513.
(13) Winey, K. I.; Laurer, J. H.; Kirkmeyer, B. P. *Macromolecules* **1998**, *33*, 507–513.
(14) Arai, K.; Eisenberg, A. *J. Macromol. Sci., Part B: Phys.* **1980**, *17*, 803–832.
(15) Yano, S.; Fujiwara, Y.; Kato, F.; Aoki, K.; Koizumi, N. *Polym. J.* **1981**, *13*, 283–291.
(16) Atorngitjawat, P.; Klein, R. J.; Runt, J. *Macromolecules* **2006**, *39*, 1815–1820.
(17) Atorngitjawat, P.; Runt, J. *Macromolecules* **2007**, *40*, 991–996.
(18) Castagna, A.; Wang, W.; Winey, K. I.; Runt, J. *Macromolecules* **2010**, *43*, 10498–10504.
(19) Heiney, P. A. *Commission on Powder Diffraction Newsletter* **2005**, *32*, 9–11.
(20) Kinning, D. J.; Thomas, E. L. *Macromolecules* **1984**, *17* 1712–1718.
(21) Benetatos, N. M.; Heiney, P. A.; Winey, K. I. *Macromolecules* **2006**, *39*, 5174–5176.
(22) van Turnhout, J.; Wubbenhorst, M. *J. Non-Cryst. Solids* **2002**, *305*, 50–58.
(23) Wubbenhorst, M.; van Turnhout, J. *J. Non-Cryst. Solids* **2002**, *305*, 40–49.
(24) Zundel, G. *Hydration and Intermolecular Interaction: Infrared Investigations with Polyelectrolyte Membranes*; Academic Press: New York, 1969.
(25) Zhou, N. C.; Burghardt, W. R.; Winey, K. I. *Macromolecules* **2007**, *40*, 6401–6405.
(26) Benetatos, N. M.; Chan, C. D.; Winey, K. I. *Macromolecules* **2007**, *40*, 1081–1088.
(27) Ayyagari, C.; Bedrov, D.; Smith, G. D. *Macromolecules* **2000**, *33*, 6194–6199.
(28) Wang, W.; Chan, T.-T.; Perkowski, A. J.; Schlick, S.; Winey, K. I. *Polymer* **2009**, *50*, 1281–1287.
(29) Eisenberg, A.; Hird, B.; Moore, R. B. *Macromolecules* **1990**, *23*, 4098–4107.
(30) Santangelo, P. G.; Roland, C. M. *Macromolecules* **1998**, *31*, 4581–4585.
(31) Glatz-Reichenbach, J. K. W.; Sorriero, L.; Fitzgerald, J. J. *Macromolecules* **1994**, *27*, 1338–1343.
(32) Kremer, F.; Schonhals, A. *Broadband Dielectric Spectroscopy*; Springer-Verlag: Berlin, 2003.
(33) North, A. M.; Pethrick, R. A.; Wilson, A. D. *Polymer* **1978**, *19*, 913–922.
(34) Yaws, C. L. *Chemical Properties Handbook*; McGraw-Hill: 1999.